Modelling, Measurement and Control A
Vol. 91, No. 3, September, 2018, pp. 95-103
Journal homepage: http://iieta.org/Journals/MMC/MMC_A

Modeling of semiconductors refractive indices using hybrid chemometric model

Luqman E. Oloore[1,3], Taoreed O. Owolabi[2,3,6*], Sola Fayose[2], Muideen Adegoke[4], Kabiru O. Akande[5], Sunday O. Olatunji[6]

[1] Department of Physics and Engineering Physics, Obafemi Awolowo University, Ile-Ife A234, Nigeria
[2] Physics and Electronics Department, Adekunle Ajasin University, Akungba Akoko 342111, Nigeria
[3] Physics Department, King Fahd University of Petroleum and Minerals, Dhahran 34464, Saudi Arabia
[4] Department of System Engineering, King Fahd University of Petroleum and Minerals, Dhahran 34464, Saudi Arabia
[5] Institute for Digital Communications, School of Engineering, University of Edinburgh, Edinburgh, Postal code EH8 9AB, United Kingdom
[6] Computer Science Department, College of Computer Science and Information Technology, Imam Abdulrahman Bin Faisal University, Dammam 31433, Saudi Arabia

Corresponding Author Email: owolabi@kfupm.edu.sa

https://doi.org/10.18280/mmc_a.910301

Received: 12 August 2018
Accepted: 20 September 2018

Keywords:
support vector regression, gravitational search algorithm, energy gaps, refractive indices and hybrid intelligent

ABSTRACT

A support vector regression (SVR)-based model and its hybrid (HSVR), both optimized with gravitational search algorithm (GSA), for accurate estimation of refractive indices of semiconductors using their energy gaps as descriptors are presented. The proposed GSA-HSVR model demonstrates a better predictive and generalization ability than ordinary GSA-SVR model. The performances of the proposed models are compared with the existing Moss and Ravindra's models and a better agreement with the experimental values were observed coupled with lowest mean absolute error of GSA-HSVR model. Considerable high coefficient of correlation and very small root mean square error also characterize GSA-HSVR model. The proposed GSA-HSVR model proves its identity and effectiveness compared to existing predictive models, in terms of accuracy, using simply accessible descriptor. It also reduces the estimation challenges accompanying determination of refractive indices of semiconductors.

1. INTRODUCTION

The evolution of modern technology aids novel semiconductors with established or promising optoelectronic properties to find wide range of applications in devices like laser diodes (LD), light emitting diodes (LED), nanotechnology, photonics, integrated circuits (IC) and other optoelectronic devices [1–3, 45]. Energy gap and index of refraction are the two fundamental properties that determine the optical and electronic properties of semiconductors. The energy gap is determined by the threshold of photon absorption while refractive index is, in general, a measure of transparency of the material to the incident light. The roles played by these two optoelectronic quantities in the study of semiconductor band structures make the correlation between the two an important part of intensive research from the last few decades [4–19]. Furthermore, it has been established that some electronic properties of a material, such as polarizability and electric permittivity, depends on the refractive index which can be calculated from the knowledge of energy gap. Also, these two basic parameters of a semiconductor are believed to have correlation since the refractive index of a material decreases with energy gap and vice versa [19].

There have been several attempts to establish a suitable relation, empirical and/or semi empirical, between the energy gap and refractive index of semiconductor materials [1, 4–19]. Many empirical formulations propose direct relationship between the energy gap and the refractive index while some relations suggest that the energy gap be calculated from electronegativity which is then used to determine the refractive index. With an assumption that the valence and conduction bands are approximately parallel to each other along the symmetry directions, Ravindra and his fellow researchers [8], [18] proposed a linear relation between refractive index and energy gap. The concept of Ravindra is believed to be an approximate Penn model. Penn model is a simple model for isotropic system which provides reasonable application to liquid and amorphous semiconductors [10]. Moss used the basics of photoconductivity to establish a relation in which the electron energy levels are scaled down by a factor of $1/\epsilon 2$ where ϵ represents the effective dielectric constant as felt by the electrons in the material and is approximately equal to the square of the refractive index of the material [13-14]. Lately, Kumar and Singh fitted model parameters to a few experimental energy gap and refractive indices data to establish an empirical relation for refractive index [15]. In his effort to modify the Penn model for high frequency dielectric constant, Gopal formulated a relationship between refractive index and energy gap [20]. Reddy et al. have proposed some empirical relations between the two fundamental quantities of a semiconductor for different compounds [4, 6]; meanwhile Anani and his colleagues found a formulation for refractive index of III–V semiconductors [19]. This work presents gravitational search algorithm-based hybrid support vector regression (GSA-HSVR) model with better estimation and generalization ability in comparison to already existing models. The results of the proposed model (GSA-HSVR) are closer to the experimental values than those of the existing models. This

is due to the inherent ability of the model to fully capture the non-linear relationship between energy band gap and refractive indices that has not been effectively captured by the existing theoretical models.

Support vector regression (SVR), as a computational intelligence technique, is known for robustness and has excelled in several fields of applications due to its unique features [21]. The uniqueness of SVR includes generalization of error-bound and non-convergence to local minimum. SVR has been employed for several applications in various research fields especially where experimental data are rarely available, such as condensed matter physics [22-24]. Its importance has been demonstrated in estimation of the properties of perovskite [25], of superconducting properties, [26-28] and surface properties of materials [29-31]. SVR uses kernel trick to handle non-linear problems. Kernel trick allows data transformation into high dimensional space with the use of mapping function called kernel function. Proper selection of hyper-parameters, such as regularization, kernel option and epsilon govern the predictive strength of SVR-based model [32]. SVR hyper-parameters are optimized in this work using a novel optimization technique, gravitational search algorithm (GSA). The GSA is a population-based optimization algorithm that works on the principle of Newtonian gravitation and laws of motion [33, 46-47]. Its excellent performance has been demonstrated in various practical applications [34-35]. In order to fully capture the complex and non-linear relationship between energy band gap and refractive indices of semiconductors, homogenously hybridized SVR (HSVR) is developed. HSVR involves hybridization of two SVR algorithms in which the outputs (estimated refractive indices) of the first SVR algorithm serve as the descriptor to the second SVR algorithm. This proposed model (HSVR) outperforms ordinary SVR in its estimates. Hybrid SVR has been previously considered for semiconductors band gap estimation [36]. However, given the importance of semiconductor applications and its monumental impact in revolutionizing the computing process coupled with significance of refractive indices to these applications, this present work applies hybrid HSVR for refractive indices estimation and the obtained result outperforms the existing models in this area of study. The outstanding performance of the proposed hybrid model shows its potential to replace the existing methods, circumvents experimental stress and ultimately eases the refractive indices determination while experimental precision is preserved.

Results of the proposed GSA-HSVR model show appreciable accuracy, based on coefficient of correlation between estimated and experimental refractive indices. A small value of mean absolute error (0.176eV) and root mean square error (0.213eV) are also observed during modeling and simulation. The estimated refractive indices for various semiconductors agree excellently with the experimental results, thus suggesting high predictive and generalization ability of the proposed models.

2. THEORETICAL BACKGROUND

This section presents the mathematical formulation of support vector regression and the proposed homogenously hybridized support vector regression model. Physical description of the optimization technique (GSA) is also presented. The parameters used for evaluating the generalization and predictive capacity of the models are also discussed.

2.1 Mathematical formulation of support vector regression (SVR)

SVR is a machine learning tool that uses statistical learning principle to form unique pattern between descriptors and desired targets [1]. The statistical learning principles are developed from structural risk minimization theory [5-6]. SVR algorithm locates minimum possible error within a certain distance in the training data using ε − insensitive loss function [7]. Unlike support vector machine, which is meant for classification problems, SVR employs kernels; and this has contributed to its uniqueness. For instance, for energy band gap descriptor E, a decision refractive indices function $\mu(\omega, E)$ which allows mapping of the descriptor is given in the equation (1), where $\langle \omega, E \rangle$ represents the inner product while ω is a weight vector.

$$\mu(\omega, E) = \langle \omega, E \rangle + b \tag{1}$$

where $b \in \mathbb{R}$

In the SVR algorithm, flatness of the generated function is ensured through Euclidian norm minimization; that is by subjecting $\frac{1}{2}\|\omega\|^2$ to the following condition as described in Ref. [8].

$$\mu_i - \langle \omega, E \rangle - b \leq \varepsilon \text{ and } \langle \omega, E \rangle + b - \mu_i \leq \varepsilon \tag{2}$$

where μ_i represents the experimentally measured refractive indices of semiconductors.

It is essential to introduce slack variables, say (ξ_i, ξ_i^*), to create room for infeasible constraints; and hence, the optimization problem is modified as presented in the equation (3).

$$\frac{1}{2}\|\omega\|^2 + C\sum_{i=1}^{n}(\xi_i + \xi_i^*) \tag{3}$$

where C is the regularization factor and n the number of data points. Equation (4) presents the optimization problem with inclusion of slack variables.

$$\mu_i - \langle \omega, E_i \rangle - b \leq \varepsilon + \xi_i \; \langle \omega, E_i \rangle + b - \mu_i \leq \varepsilon + \xi_i^* \tag{4}$$

Proper handling of the optimization problem is ensured by introduction of Lagrange multipliers, λ_i and λ_i^*, described in Ref. [9]. Equation (5) represents the new refractive indices decision function in term of the Lagrange multipliers and the kernel function.

$$\mu(\lambda, E) = \sum_{i=1}^{n}(\lambda_i - \lambda_i^*)\, g\langle E_i, E \rangle + b \tag{5}$$

$g\langle E_i, E \rangle$ represents the kernel function. Various kernel functions were tested during the process of optimizing the SVR hyper-parameters, using gravitational search (GSA) algorithm; the non-linear mapping that provides the optimum performance to the proposed model is the Gaussian kernel function presented in equation (6).

$$g\langle E_i, E \rangle = exp\left(-\left(\frac{\|E_i - E\|}{\alpha^2}\right)^2\right) \tag{6}$$

The parameter α in equation (6) is the kernel option that needs to be tuned using GSA algorithm. Estimation accuracy of the model is determined by the value of the various SVR hyper-parameters namely: Gaussian kernel option, loss function, lambda hyper-parameter and regularization factor [7]. Kernel option refers to the parameter of kernel function that controls the transformation of data-points to the space with high dimension, while lambda hyper-parameter sorts for hyper-plane where attainment of minimum possible error is most probable [9]. The penalty factor maintains the tradeoff between flatness of the decision function and the level to which deviation lager than the specified threshold (epsilon) is tolerated.

2.2 The proposed homogeneously hybridized support vector regression (HSVR)

Homogenously hybridized support vector regression (HSVR) is a class of hybrid intelligent proposed recently for solving complex problems that cannot be handled by ordinary SVR-based model to the desired level of accuracy [10-11]. It utilizes the desired features of two SVR algorithms for improved performance. In its operation, the energy band gap (descriptor) of semiconductors are fed into first SVR algorithm for refractive indices estimation while the estimated refractive indices emanating from the first SVR algorithm serve as the input to the second algorithm for its estimation. The descriptor in the first stage of the HSVR has been transformed into a new descriptor that contains all the intricacies, patterns and other information necessary for accurate estimation of refractive index of the material. The second SVR model now has access to a pool of information rich enough to develop a more efficient model. The resulting homogeneous SVR–SVR hybrid system minimizes generalized error bound more than once; and this results in an improved performance over the single SVR-based system. Among the advantages of the proposed hybridization is that it aggregates intrinsic features of two different SVR algorithms and allow the utilization of kernels of different parameters for data transformation. The regression functions of the initial and final stage of the proposed HSVR model are presented in equation (7) and (8) respectively assuming $\mu(E) = Y$.

$$\mu(E) = \sum_{i=1}^{N_{\text{support vectors}}} \left(\lambda_i - \lambda_i^*\right) \exp\left(-\frac{\left\|E_i - E\right\|^2}{\sigma^2}\right), 0 \le \lambda_i^* < C, 0 \le \lambda_i \le C \tag{7}$$

$$R(y) = \sum_{j=1}^{N} \left(\eta_j - \eta_j^*\right) \exp\left(-\frac{\left\|y_j - y\right\|^2}{\sigma^2}\right), 0 \le \eta_j^* < C, 0 \le \eta_j \le C \tag{8}$$

where N is the number of support vectors while η and η^* are the Lagrange multipliers

2.3 Optimization algorithm: The Gravitational Search Algorithm (GSA)

Gravitational search algorithm (GSA) is a recently developed search heuristic algorithm whose working principle is based on Newton's law of gravitation and the equations of motion [12]. The algorithm considers the objects in Newtonian description as agents whose mass determines the actual performance. In principle, the gravitational force brings about global movement towards massive agents. Each of the agent has characteristic position (R), inertial mass (M_i), active gravitational mass (M_a) and passive gravitational mass (M_p). Strength of gravitational field of an agent is a measure of its M_a while the resistance to change of state of motion, due to the force experienced, is determined by the M_i, and the M_p measures the strength of the interaction between the agent and the field. Fitness function is used to determine the inertial mass of each agent; and their respective position is consequently updated [13-14].

As stated earlier, the entire GSA can be considered as an isolated system of masses governed by Newton's law of gravitation and the equations of motion. Let the position of jth agent in a system of N agents be defined by equation (9).

$$R_j = \left(r_j^1, r_j^2, \dots, r_j^d\right) \text{ where } j = 1, 2, \dots, N \tag{9}$$

where r_j^d is the position of jth agent in the dth dimension.

Let the Euclidean distance between mass M_{pj} and M_{ak} be $X_{jk}(t) = \left\|R_j(t), R_k(t)\right\|$, the gravitational attractive force between mass M_{pj} and mass M_{ak} is

$$F_{jk}^d(t) = G(t) \frac{M_{pj}(t) M_{ak}(t)}{X_{jk}(t) + \varepsilon^*} \left\{r_k^d(t) - r_j^d(t)\right\} \tag{10}$$

And

$$G(t) = G(t_0) \left(\frac{t_0}{t}\right)^{\nu} \qquad \nu < 1 \tag{11}$$

Equation (11) represents the time dependent gravitational constant whose value decreases with time. The acceleration $\left(a_j^d(t)\right)$ of the jth agent, whose inertia mass is M_{ij}, in the dth dimension at time t is given by the Equation (12), with the stochastic feature imposed through Equation (13).

$$a_j^d(t) = \frac{F_j^d(t)}{M_{ij}} \tag{12}$$

$$F_j^d(t) = \sum_{k=1, k \ne j}^{N} rand_k F_{jk}^d(t) \tag{13}$$

In the Equation (13), $rand_k$ represents a random number, which enforces randomness to the search procedure and ensures the ultimate location of the optimum SVR hyper-parameters; it spans through [0, 1] interval.

The next velocity of an agent is determined from its acceleration and some fraction of its present velocity. Thus, velocity and position of the agent are updated per the equations (14) and (15) respectively.

$$v_j^d(t+1) = rand_k v_j^d(t) + a_j^d(t) \tag{14}$$

$$x_j^d(t+1) = x_j^d(t) + v_j^d(t+1) \tag{15}$$

The inertial and gravitational masses are, of course, updated each time; by using the following Equations:

$$m_j(t) = \frac{fit_j(t) - worst(t)}{best\ (t) - worst\ (t)} \tag{16}$$

And

$$M_j(t) = \frac{m_j(t)}{\sum_{k=1}^{N} m_j(t)} \quad (17)$$

where $fit_j(t)$ represents fitness of the jth agent at time t and the assumption given by equation (18) was adopted.

$$M_{aj} = M_{pj} = M_{ij}, \quad j = 1, 2, \ldots, N \quad (18)$$

Besides the inertial and gravitational masses, the fitness function helps in determining a more efficient agent (that is the one with heavier mass) which moves sluggishly due to its comparatively large attractive gravitational force.

2.4 Accuracy evaluation of the proposed gsa-svr and gsa-hsvr model

The degree of accuracy and precision of the proposed GSA-SVR and the GSA-HSVR models in predicting the refractive indices of various semiconductor materials were analyzed by calculating the correlation coefficient (CC), mean square error (RMSE), and mean absolute error (MAE). The formulations for CC, RMSE and MAE are given by Equations (19), (20) and (21) respectively.

$$cc = \frac{\sum_{i=1}^{n} \left(\mu_i^{est} - \bar{\mu}^{est}\right)^2}{\sum_{i=1}^{n} \left(\mu_i^{exp} - \bar{\mu}^{exp}\right)^2} \quad (19)$$

$$RMSE = \sqrt{\frac{\sum_{i=1}^{n} \left(\mu_i^{est} - \bar{\mu}^{est}\right)^2}{n}} \quad (20)$$

$$MAE = \frac{\sum_{i=1}^{n} \left|\mu_i^{est} - \bar{\mu}^{est}\right|}{n} \quad (21)$$

μ_i^{est} and μ_i^{exp} in the equations respectively represent values of the estimated refractive index and the experimental refractive index while $\bar{\mu}^{est}$ and $\bar{\mu}^{exp}$ represent their respective means. The number of data samples is denoted by n.

3. DEVELOPMENT OF GSA-SVR AND GSA-HSVR MODELS

This section presents the computational methodology employed while developing GSA-SVR and GSA-HSVR models. The computational flow chat of the proposed model is also presented. The data-set used for the modeling and simulation is analyzed statistically and the outcomes of the analysis are discussed.

3.1 Description of dataset

The descriptors used in estimating the refractive index of the semiconductor materials are the band gap energy of the respective materials. The models, GSA-SVR and GSA-HSVR, are developed by adopting test-set cross validation methods using eighty-five experimental band gap energies. The data are culled from [15-16]. Statistical analysis was performed on the dataset, and the results are as presented in table I. The results of the mean and standard deviation presented in the table I can be used to deduce the consistency in the dataset. The results of the statistical analysis give us an insight to the data and its strength for the proposed estimation.

Table 1. Results of statistical analysis

	E_g (eV)	Refractive indices
Mean	2.92	2.79
Maximum	10.5	5.73
Minimum	0.00	1.33
Standard deviation	2.77	0.88

3.2 Computational description of the proposed hybrid models

The proposed GSA-HSVR model is developed within the MATLAB computing environment. The data was randomized and partitioned into two namely; training dataset and testing dataset in the ratio 80 to 20, respectively. The training dataset consists of the band gap energies (Eg) of semiconductor materials and their corresponding refractive index (μ) to train the model; also, the testing dataset is composed of Eg and their respective μ for testing the model. Gravitational search algorithm (GSA) was adopted for SVR hyper-parameters optimization while the RMSE between the measured refractive indices and the estimated values serves as the fitness function. The procedures for computational hybridization of GSA and SVR algorithms are itemized as follows;

Step I: *Data partitioning:* The available data for simulation was randomly separated into training and testing portion in the ratio of 80 to 20. This means that sixty-eight and seventeen data points were respectively used for training and testing purposes.

Step II: *Initialization of GSA agents*: population of agents in GSA description was initialized with each agent encodes SVR hyper-parameters which include regularization factor (C), epsilon (ε) and kernel option (α)

Step III: With each agent of the population, root mean square error (RMSE) between the experimentally measured refractive indices and the estimated values was minimized using training data set as follows:

(1) SVR hyper-parameters encoded in each of the agent was used to train SVR algorithm with the aid of training dataset and root mean square error (which serves as the fitness function) of each of the agent was obtained using testing data-set.

(2) Using the fitness of each of the agent coupled with the fitness of the entire population, gravitational mass of each of the agent was computed using equations (16) and (17) while the assumption contained in equation (18) was also implemented.

(3) Gravitational pull on each of the agents due to the presence of other agents was computed using equations (11) and (13).

(4) Accelerations of the agents were computed using equation (12)

(5) Velocities and Positions of the agents were updated and the process continues until the root mean square errors (for testing data-set) between the experimental values of refractive indices and estimated refractive indices converge to global minimum.

Step IV: The SVR hyper-parameters that minimize RMSE were used to develop GSA-SVR model

Step V: Development of GSA-HSVR went a step further by

incorporating another SVR algorithm into the described GSA-SVR model. The estimated refractive indices obtained through Step I to Step III were fed into another SVR algorithm and Step I to Step III were repeated for another set of GSA agents. Algorithm1 shows the computational description of the proposed model.

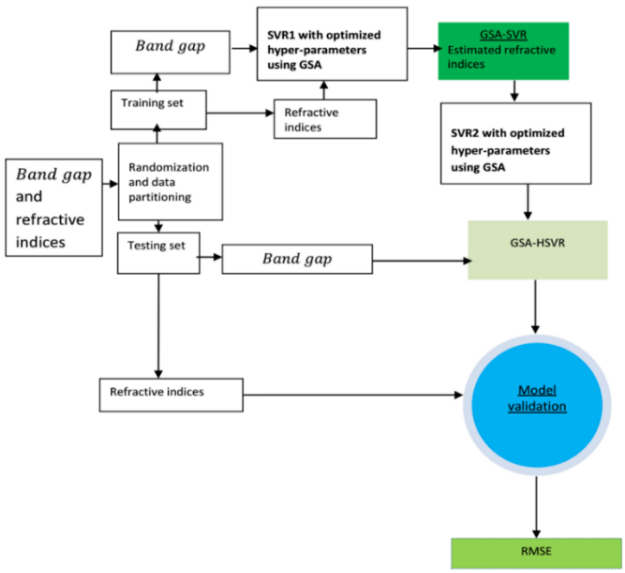

Algorithm 1. The computational description of the proposed model

4. RESULTS AND DISCUSSION

This section presents the results of the developed models (GSA-SVR and GSA-HSVR). The correlation cross-plot between experimentally measured refractive indices and the estimated values are presented and discussed. The comparison between the results of the developed model and the existing theoretical models are also presented and discussed.

4.1 Performance sensitivity of the proposed models to the initial population of the agents

The exploration and exploitation ability of GSA based model can be influenced by the number of initial population of the agents. For a small number of agents, the search space might not be efficiently explored by the agents and convergence to local minimum would be observed.

Similarly, for a very large number of agents exploring a search space, the exploration ability of the algorithm is strengthened while complexity might set in when large number of agents are exploiting for global minimum. In order to maintain a balance between exploration and exploitation ability of the model, the influence of the number of agents on the performance of the model is investigated and presented in Fig.1 and Fig.2 for GSA-SVR and GSA-HSVR model respectively. Fig. 1 presents the performance sensitivity of the proposed GSA-SVR model to the number of agents, as measured based on the RMSE. As can be observed from the figure, performance sensitivity was investigated when the number of agents was 10, 20, 40 and 60 respectively. It was observed that a minimum error, which may be regarded as the local minimum, was recorded when the number of agents was 10. Whereas an initial population of 50 agents gives the global minimum with a RMSE value of about 0.2936. Above this optimum number of agents, further increase in the number of agents leads to convergence to local minimum due to the complexity as large number of agents is exploiting a global minimum. Similarly, Fig. 2 depicts the results of measurement of the performance sensitivity of GSA-HSVR model. It is observed that a local minimum arises when the number of agents was 40; this almost overlaps with the population containing 10 agents. Also, the global minimum was achieved with initial population of 20 agents which corresponds to a RMSE value of 0.2128. The optimum values of SVR hyper-parameters for both GSA-SVR and GSA-HSVR model including the optimum number of agents are presented in table 2.

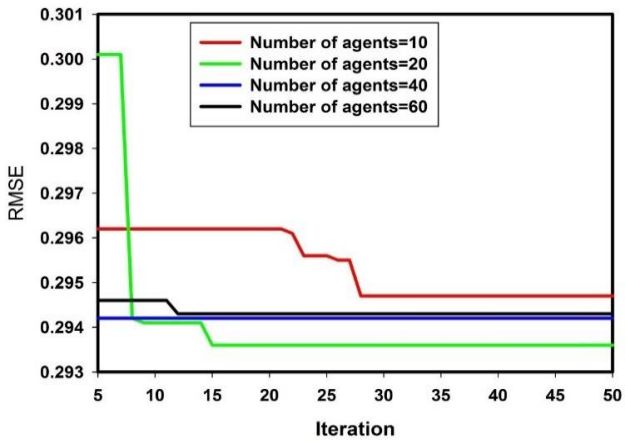

Figure 1. Sensitivity of the developed GSA-SVR model to the number of agents

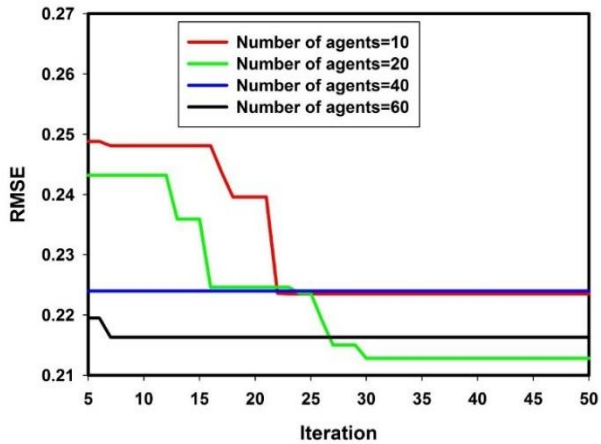

Figure 2. Sensitivity of the developed GSA-HSVR model to the number of agents

Table 2. Optimum hyper-parameters values as obtained by GSA

Hyper parameter	GSA-SVR	GSA-HSVR
Regularization factor (C)	695.6935	513.7134
Epsilon	0.0582	0.0022
Kernel option	0.5	0.2848
Lambda	0.1	e-7
Kernel function	Gaussian	Gaussian

4.2 Comparison of the estimation and generalization ability of ordinary SVR and the proposed hybrid system (HSVR)

Cross-plots of the estimated and experimental values of the refractive indices of semiconductor materials, using GSA-SVR model, for both training and testing datasets are as shown in Fig. 3. The alignment of the data-points with little deviation shows presence of only small discrepancies between the estimated and experimental refractive indices for training and testing set of data. The deviation between experimental and estimated refractive indices for both training and testing data-set is around 8% in both cases. Meanwhile, similar cross-plot, using GSA-HSVR, is depicted in Fig. 4 with smaller discrepancies between the experimental and estimated indices of refraction. In the GSA-HSVR model, less than 7% deviation was observed for the training set while the deviation in the testing set is less than 4%. The small deviations, along with the small RMSE values, shows closeness of the estimated and experimental values of the refractive indices of the semiconductors, and justify the effectiveness of the proposed models.

Fig. 5 presents the performance comparison between GSA-SVR and GSA-HSVR models on the basis of correlation coefficient (CC). Other determinants of estimation accuracy, for the models, depicted by Fig.6 and Fig.7, are RMSE and MAE respectively. The results of the training and testing phase of GSA-SVR model are very close to each other with just about 0.08% improvement in the result of the testing dataset. On the other hand, the generalization capacity of GSA-HSVR model to unseen dataset during the testing stage outperforms the training phase by 4.7%. Comparison between the results of training phase of GSA-SVR and GSA-HSVR model, as depicted in Fig.5, shows that GSA-HSVR outperforms ordinary GSA-SVR model by 1.28%. Similar improvement of about 4.7% was also observed during testing phase of the simulation. The observed performance improvement demonstrated by GSA-HSVR model can be attributed to the ability of the hybrid model to minimize the generalization error bound more than once as well as multiple transformations of input data to high feature space.

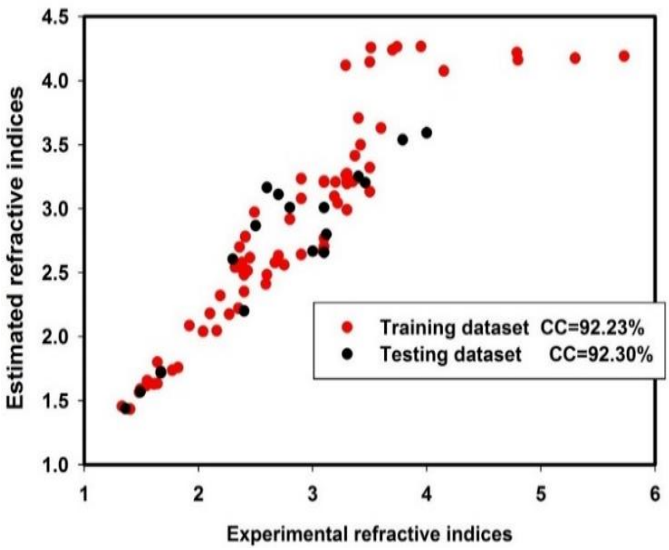

Figure 3. Correction crossplot between the experimental and estimated refractive indices of semiconductors using GSA-SVR model

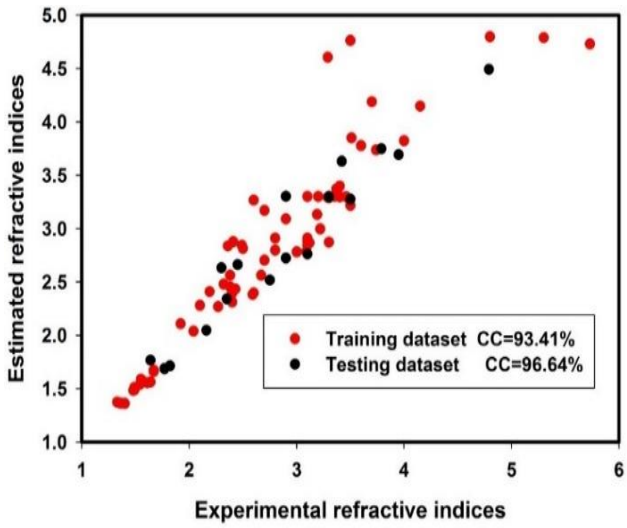

Figure 4. Correction crossplot between the experimental and estimated refractive indices of semiconductors using GSA-HSVR model

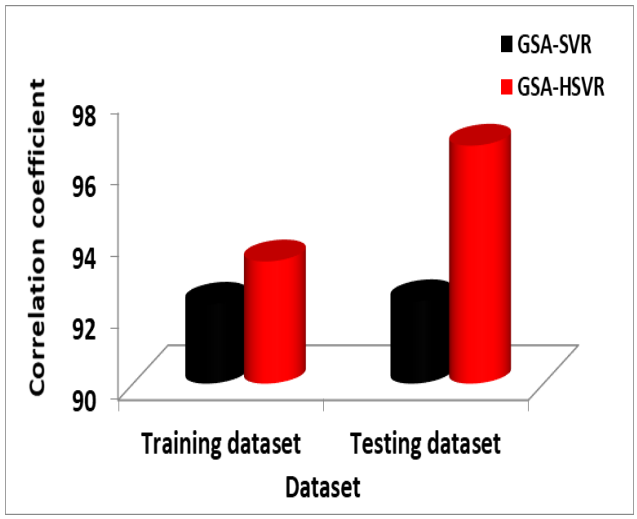

Figure 5. Generalization and predictive capacity of GSA-SVR and GSA-HSVR models on the basis of correlation coefficient

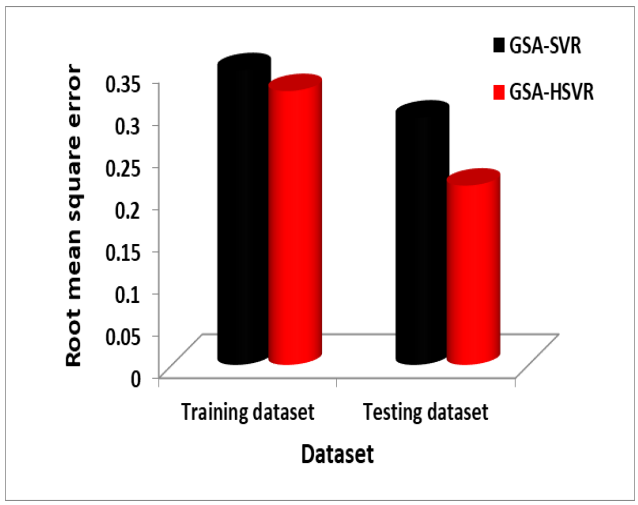

Figure 6. Generalization and predictive capacity of GSA-SVR and GSA-HSVR models on the basis of root mean square error

Fig.6 and Fig.7 compares the generalization and predictive ability of GSA-SVR and GSA-HSVR models on the basis of RMSE and MAE, respectively. The RMSE values for training and testing phase of GSA-SVR-based model are 0.3498 and 0.2936 respectively, as in Table 3. Whereas, for the GSA-HSVR-based model the RMSE values for training and testing stages are 0.3250 and 0.2128 respectively; this is about 28.6 % less than the RMSE obtained for the testing stage of GSA-SVR model. Also, the MAE is reduced, by 30.5 %, from 0.2537 to 0.1763. Table 3 contains list of the actual values of the determinant of future estimation accuracy of the proposed models.

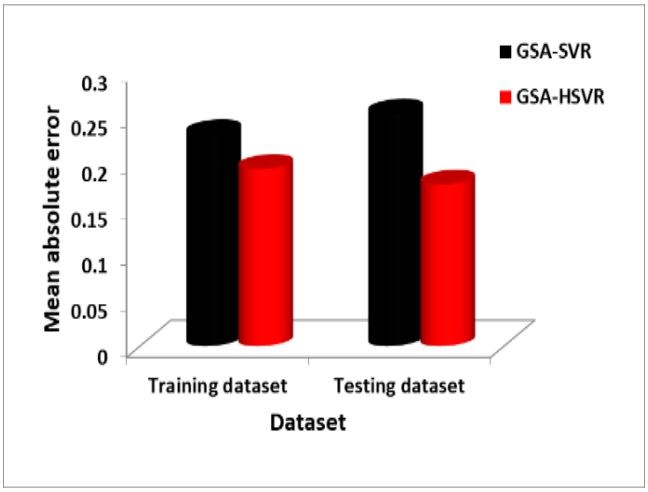

Figure 7. Generalization and predictive capacity of gsa-svr and gsa-hsvr models on the basis of mean absolute error

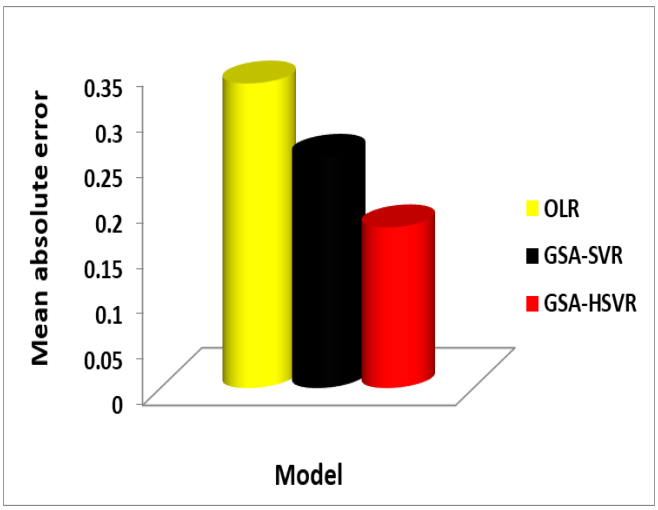

Figure 8. Comparing the mean absolute error (MAE) of OLR, GSA-SVR and GSA-HSVR models

4.3 Comparison of predictive capacity of the developed model with ordinary regression model

The predictive and generalization capacity of the developed models (GSA-SVR and GSA-HSVR) are compared with that of ordinary linear regression (OLR) on the basis of mean absolute error obtained using testing dataset. The OLR model obtained using the training dataset is shown in equation (23) as.

$$R = -0.2463E_g + 3.4823 \qquad (23)$$

R and E_g are the refractive index and energy band gap, respectively

Table 3. Measure of estimation accuracy of the gsa-svr and gsa-hsvr models

	GSA-SVR		GSA-HSVR	
	Training dataset	testing dataset	Training dataset	testing dataset
RMSE	0.3498	0.2936	0.325	0.2128
MAE	0.2312	0.2537	0.1932	0.1763
CC	92.23	92.3	93.41	96.64

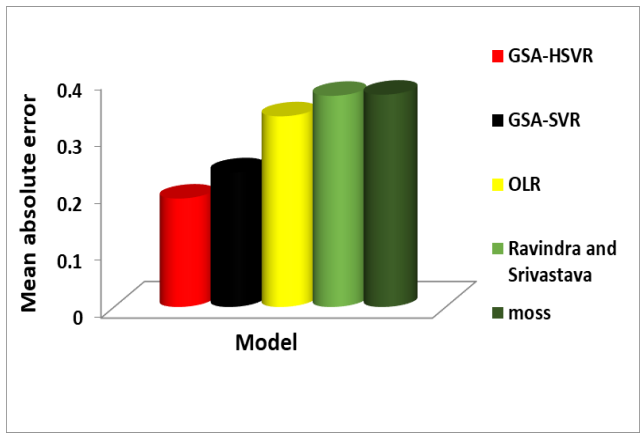

Figure 9. Comparing the mean absolute error (mae) for gsa-svr and gsa-hsvr models with other theoretical models

Using the testing dataset, the mean absolute error performance of OLR model is compared to that of the developed GSA-SVR and GSA-HSVR model and the result is depicted in. Fig.8. The significance of non-linear modeling in estimating the refractive indices of semiconductors manifests from performance comparison between the models as both the developed non-linear models greatly perform better than the OLR. In comparison to OLR, Figure 8 shows that both the GSA -SVR and GSA-HSVR results in error performance improvement of 24.06% and47.23%, respectively. This result justifies the consideration of non-linear modeling techniques in this work.

4.4 Comparison of the determinant of estimation accuracy of the developed model with other existing theoretical models

In order to further validate the predictive and generalization strength of the developed models, the developed models were utilized for estimating the refractive indices of some semiconductors. In the implementation, the models were only supplied with the descriptors while the developed model utilized the acquired support vectors during the training stage for its refractive indices estimation. The mean absolute error of GSA-SVR and GSA-HSVR models are compared with that of other existing theoretical models using the same data-points and presented in table 4 as well as Fig.9. The developed GSA-HSVR model has the least mean absolute error of 0.190 followed by the GSA-SVR model whose mean absolute error value is 0.236; the models developed by Ravindra and Moss have mean absolute error of 0.370 and 0.372 respectively. Table 4 presents summary of mean absolute error for the compared models. The smallest mean absolute error

demonstrated by the developed GSA-HSVR-based model shows its superiority over the existing predictive models.

5. CONCLUSIONS

Gravitational search algorithm-based support vector regression (GSA-SVR) model and its hybrid (GSA-HSVR) are presented for semiconductors refractive indices estimation. The GSA-SVR-based model is characterized with a high CC of 92.30 %, small MAE of 0.254 and RMSE of 0.294. However, the GSA-HSVR-based model shows better generalization and predictive capacity with CC, MAE and RMSE of 96.64 %, 0.176 and 0.213, respectively. On the basis of RMSE and MAE, GSA-HSVR model outperforms GSA-SVR model with performance improvement of 28.6% and 30.5%, respectively. The generalization and predictive capacities of GSA-SVR and GSA-HSVR model are better than other existing theoretical model such as Ravindra and Moss model when compared on the basis of mean absolute error. The outstanding performance of the developed GSA-HSVR based model makes it a viable model through which refractive indices of semiconductor materials can be predicted with high precision and accuracy.

ACKNOWLEDGMENT

The contribution of Akande O Kabiru is acknowledged.

REFERENCES

[1] Tripathy SK. (2015). Refractive indices of semiconductors from energy gaps. Opt. Mater. (Amst). 46: 240–246. http://dx.doi.org/10.1016/j.optmat.2015.04.026

[2] Paskov PP. (1997). Refractive indices of InSb, InAs, GaSb, InAs[sub x]Sb[sub 1−x], and In[sub 1−x]Ga[sub x]Sb: Effects of free carriers. J. Appl. Phys 81(4): 1890.

[3] Rappl PHO, McCann PJ. (2003). Development of a novel epitaxial-layer segmentation method for optoelectronic device fabrication. IEEE Photonics Technol. Lett 15(3): 374–376.

[4] Reddy RR. et al. (2008). Correlation between optical electronegativity and refractive index of ternary chalcopyrites, semiconductors, insulators, oxides and alkali halides. Opt. Mater. (Amst) 31(2): 209–212. http://dx.doi.org/10.1016/j.optmat.2008.03.010

[5] Reddy RR, Nazeer Ahammed Y. (1995). A study on the Moss relation. Infrared Phys. Technol 36(5): 825–830. http://dx.doi.org/10.1016/1350-4495(95)00008-M

[6] Reddy et al. (2009). Interrelationship between structural, optical, electronic and elastic properties of materials. J. Alloys Compd. 473(1): 28–35. http://dx.doi.org/10.1016/j.jallcom.2008.06.037

[7] Reddy RR, Anjaneyulu S. (1992). Analysis of the moss and ravindra relations. Phys. status solidi 174(2): K91–K93. http://dx.doi.org/10.1002/pssb.2221740238

[8] Ravindra NM, Auluck S, Srivastava VK. (1979). On the penn gap in semiconductors. Phys. Status Solidi 93(2): K155–K160. http://dx.doi.org/10.1002/pssb.2220930257

[9] Ravindra NM, Ganapathy P, Choi J. (2006). Energy gap–refractive index relations in semiconductors – An overview. http://dx.doi.org/10.1016/j.infrared.2006.04.001

[10] Penn DR. (1962). Wave-number-dependent dielectric function of semiconductors. Phys. Rev. 128(5): 2093–2097.

[11] Pal S, Kumar Tiwari R, Chandra Gupta D, Singh Verma A. (2014). Simplistic theoretical model for optoelectronic properties of compound semiconductors. J. Mater. Phys. Chem. 2(2): 20–27.

[12] Moss, Smoluchowski R. (1954). Photoconductivity in the elements. Phys. Today 7(2): 18.

[13] Moss TS. (1985). Relations between the refractive index and energy gap of semiconductors. Phys. status solidi 131(20): 415–427.

[14] Moss TS. (1950). A relationship between the refractive index and the infra-red threshold of sensitivity for photoconductors. Proc. Phys. Soc. Sect. B 63(3):167–176.

[15] Kumar V, Singh JK. (2010). Model for calculating the refractive index of different materials. IJPAP 48(8).

[16] Kumar V, Sinha A, Singh BP, Sinha AP, Jha V. (2015). Refractive index and electronic polarizability of ternary chalcopyrite semiconductors. Chinese Phys. Lett 32(12): 127701.

[17] Hervé PJL, Vandamme LKJ. (1995). Empirical temperature dependence of the refractive index of semiconductors. J. Appl. Phys. 77(10): 5476.

[18] Gupta VP, Ravindra NM. (1980). Comments on the moss formula. Phys. status solidi 100(2): 715–719.

[19] Anani M, Mathieu C, Lebid S, Amar Y, Chama Z, Abid H. (2008). Model for calculating the refractive index of a III–V semiconductor. Comput. Mater. Sci 41(4): 570–575.

[20] Blakemore JS. (1982). Semiconducting and other major properties of gallium arsenide. J. Appl. Phys. 53(10): R123. http://dx.doi.org/10.1063/1.331665

[21] Akande KO, Owolabi TO, Olatunji SO, AbdulRaheem A. (2016). A hybrid particle swarm optimization and support vector regression model for modelling permeability prediction of hydrocarbon reservoir. J. Pet. Sci. Eng 0–1 http://dx.doi.org/10.1016/j.petrol.2016.11.033

[22] Cui Y, Dy JG, Alexander B, Jiang SB. (2008). Fluoroscopic gating without implanted fiducial markers for lung cancer radiotherapy based on support vector machines. Phys. Med. Biol 53: 315–327. http://dx.doi.org/10.1088/0031-9155/53/16/N01

[23] Cai CZ, Xiao TT, Tang JL, Huang SJ. (2013). Analysis of process parameters in the laser deposition of $YBa_2Cu_3O_7$ superconducting films by using SVR. Phys. C Supercond 493: 100–103. http://dx.doi.org/10.1016/j.physc.2013.03.038

[24] Akande KO, Owolabi TO, Olatunji SO. (2015). Investigating the effect of correlation-based feature selection on the performance of support vector machines in reservoir characterization. J. Nat. Gas Sci. Eng 22: 515–522. http://dx.doi.org/10.1016/j.jngse.2015.01.007

[25] Majid A, Khan A, Javed G, Mirza AM. (2010). Lattice constant prediction of cubic and monoclinic perovskites using neural networks and support vector regression. Comput. Mater. Sci. 50: 363–372. http://dx.doi.org/10.1016/j.commatsci.2010.08.028

[26] Owolabi TO, Akande KO, Olatunji SO. (2016).

Application of computational intelligence technique for estimating superconducting transition temperature of YBCO superconductors. Appl. Soft Comput 43(2016): 143–149

[27] Akande KO, Owolabi TO, Olatunji SO. (2014). Estimation of superconducting transition temperature T C for superconductors of the doped MgB2 system from the crystal lattice parameters using support vector regression. J. Supercond. Nov. Magn. http://dx.doi.org/10.1007/s10948-014-2891-7

[28] Cai CZ, Wang GL, Wen YF, Pei JF, Zhu XJ, Zhuang WP. (2010). Superconducting transition temperature T c estimation for superconductors of the doped mgb2 system using topological index via support vector regression. J. Supercond. Nov. Magn 23(5): 745–748, Jan. 2010. http://dx.doi.org/10.1007/s10948-010-0727-7

[29] Owolabi TO, Akande KO, Olatunji SO. (2015). Development and validation of surface energies estimator (SEE) using computational intelligence technique. Comput. Mater. Sci. 101: 143–151. http://dx.doi.org/10.1016/j.commatsci.2015.01.020

[30] Owolabi TO, Akande KO, Olatunji SO. (2015). Estimation of surface energies of hexagonal close packed metals using computational intelligence technique. Appl. Soft Comput. 31: 360–368. http://dx.doi.org/10.1016/j.asoc.2015.03.009

[31] Owolabi TO, Akande KO, Sunday OO. (2015). Modeling of average surface energy estimator using computational intelligence technique. Multidiscip. Model. Mater. Struct 11(2): 284–296.

[32] Owolabi TO, Akande KO, Olatunji SO, Alqahtani A, Aldhafferi N. (2016). Estimation of curie temperature of manganite-based materials for magnetic refrigeration application using hybrid gravitational based support vector regression. AIP Adv 6(10): 105009. http://dx.doi.org/10.1063/1.4966043

[33] Rashedi E, Nezamabadi-pour H, Saryazdi S. (2009). GSA: A gravitational search algorithm. Inf. Sci. (Ny)., 179(13): 2232–2248. http://dx.doi.org/10.1016/j.ins.2009.03.004

[34] Niu P, Liu C, Li P. (2015). Optimized support vector regression model by improved gravitational search algorithm for flatness pattern recognition. Neural Comput. Appl. 2015:1167–1177

[35] Ju FY, Hong WC. (2013). Application of seasonal SVR with chaotic gravitational search algorithm in electricity forecasting. Appl. Math. Model 37(23): 9643–9651. http://dx.doi.org/10.1016/j.apm.2013.05.016

[36] Owolabi TO, Akande KO, Olatunji SO, Alqahtani A, Aldhafferi N. (2017). Modeling energy band gap of doped TiO2 semiconductor using homogeneously hybridized support vector regression with gravitational search algorithm hyper- parameter optimization, AIP Adv 115225, http://dx.doi.org/10.1063/1.5009693

[37] Owolabi TO, Zakariya YF, Akande KO, Olatunji SO. (2016). Estimation of melting points of fatty acids using homogeneously 3 hybridized support vector regression. Neural Comput. Appl., 2016

[38] Owolabi TO, Akande KO, Olatunji SO, Alqahtani A. (2016). A novel homogenous hybridization scheme for performance improvement of support vector machines regression in reservoir characterization. Appl. Comput. Intell. Soft Comput 2016: 1–10. http://dx.doi.org/10.1155/2016/2580169

[39] Drucker H, Burges CJC, Kaufman L, Smola AJ, Vapnik VN. (1996). Support vector regression machines. Adv. Neural Inf. Process. Syst 9.

[40] Basak D, Pal S, Patranabis DC. (2007). Support Vector Regression, Neural Inf. Process. – Lett. Rev 11(2007).

[41] Vapnik VN. (1995). The nature of statistical learning theory. Springer-Verlag New York, Inc. http://dx.doi.org/10.1007/978-1-4757-3264-1

[42] Owolabi TO, Akande KO, Olatunji SO. (2016). Computational intelligence method of estimating solid-liquid interfacial energy of materials at their melting temperatures. J. Intell. fuzzy Syst 31: 519–527. http://dx.doi.org/10.3233/IFS-162164

[43] Thenmozhi M, Sarath Chand G. (2016). Forecasting stock returns based on information transmission across global markets using support vector machines. Neural Comput. Appl 27: 805–824. http://dx.doi.org/10.1007/s00521-015-1897-9

[44] Verma AS, Singh RK, Rathi SK. (2009). An empirical model for dielectric constant and electronic polarizability of binary (ANB8-N) and ternary (ANB2+NC27-N) tetrahedral semiconductors. J. Alloys Compd 486(1-2): 795–800. http://dx.doi.org/10.1016/j.jallcom.2009.07.067

[45] Manukonda D, Srinivasa RG. (2018). A fuzzy logic controller based vortex wind turbine for commercial applications. Modelling, Measurement and Control A 91(2): 54-58. http://dx.doi.org/10.18280/mmc_a.910204

[46] Mehta D, Prasanta K, Anandita C. (2018). Development of energy efficient, cost-optimized transformer with low partial discharges. Modelling, Measurement and Control A 91(2): 59-65. https://doi.org/10.18280/mmc_a.910205

[47] Samala RK, Mercy RK. (2018). Optimal DG sizing and siting in radial system using hybridization of GSA and firefly algorithms. Modelling, Measurement and Control A 91(2): 77-82. https://doi.org/10.18280/mmc_a.910208